



# Estimation of Reaction Rates of Transesterification Pathways

Mario Alberto Pérez-Méndez<sup>1</sup>, Gladys Jiménez-García<sup>2</sup>, Rafael Huirache-Acuña<sup>1</sup> and Rafael Maya-Yescas<sup>1\*</sup>

<sup>1</sup>Facultad de Ingeniería Química, Universidad Michoacana de San Nicolás de Hidalgo, Morelia, México, <sup>2</sup>División de Ingeniería Biomédica, Instituto Tecnológico Superior de Pátzcuaro, Pátzcuaro, México

## OPEN ACCESS

### Edited by:

Uriel Caudillo-Flores,  
Universidad Nacional Autónoma de  
México, Mexico

### Reviewed by:

Attila Egedy,  
University of Pannonia, Hungary  
Reyna Natividad,  
Universidad Autónoma del Estado de  
México, Mexico

### \*Correspondence:

Rafael Maya-Yescas  
rmayay@umich.mx

### Specialty section:

This article was submitted to  
Chemical Reaction Engineering,  
a section of the journal  
Frontiers in Chemical Engineering

**Received:** 28 February 2021

**Accepted:** 28 May 2021

**Published:** 10 June 2021

### Citation:

Pérez-Méndez MA, Jiménez-García G,  
Huirache-Acuña R and  
Maya-Yescas R (2021) Estimation of  
Reaction Rates of  
Transesterification Pathways.  
Front. Chem. Eng. 3:673970.  
doi: 10.3389/fceng.2021.673970

Experimental estimation of reaction rates is a common aspect of reaction engineering because reaction kinetics are the base of the design of chemical reactors. However, it is not easy to follow complex reactions as it is the case of transesterification of triglycerides in presence of sodium hydroxide. Identifying the possible reaction pathways taking place as ionic and sequential, starting with the inorganic formation of methoxide, and followed by each one of the three organic transesterification steps of virgin soybean oil, deeper understanding about kinetics of this reacting path has been obtained. Reaction rate evaluations were performed by following the solution's pH, based on a  $2^{4-1}$  design of experiments, making possible to estimate the rate constants. Additionally, it was observed that there is an optimum amount of sodium hydroxide feed to the process, therefore it is possible to minimize its addition, which favors diminishing the volume of leaching water. The best yield to fatty acid methyl esters, using the minimum amount of sodium hydroxide, was 98.84 wt%, which is highly competitive.

**Keywords:** fatty acid methyl esters, ionic reactions, kinetic rates estimation, Simultaneous homogeneous reactions, triglycerides transesterification

## INTRODUCTION

Experimental estimation of reaction rates is a common aspect of reaction engineering because reaction kinetics is the base of the design of chemical reactors. However, it is not easy to follow complex reactions, as it is the case of transesterification of triglycerides in presence of sodium hydroxide. These reactions use vegetable oils and animal fats as sources of triglycerides for production of liquid fuels, fatty acid methyl esters (FAME) colloquially known as biodiesel. Four consecutive and reversible reactions are likely to occur, diglycerides (DG) and monoglycerides (MG) are intermediates formed in these reactions (Noureddini and Zhu, 1997; Silitonga et al., 2020; Mendecka et al., 2020). One of most used reacting paths is transesterification of triglycerides with methanol in presence of sodium hydroxide; the former two react to form sodium methoxide, and then this inorganic mixture is added to the triglyceride (Sharma et al., 2008; Granjo and Oliveira, 2015). Some advantages of this reacting path are moderate reaction conditions, fast and high conversion of triglycerides (around 99% at 50 min) (Marchetti et al., 2007; Vicente et al., 2004) and limited number of intermediate steps; among disadvantages is the purification of alkaline water obtained after washing the FAME produced (Betiku and Adepoju, 2013; Rincón et al., 2014; Kanna et al., 2018).

To obtain deeper understanding about this reacting path, a more robust mechanism has been proposed Mumtaz et al. (2017), identifying the possible reaction pathways taking place. In this work, the reactions are identified as ionic and sequential, starting with the inorganic formation of

**TABLE 1** | Fatty acid composition from different vegetable sources (Marchetti et al., 2007).

Vegetable oil	Fatty acid composition % by weight								
	C16:1	C18:0	C20:0	C22:0	C24:0	C18:1	C22:1	C18:2	C18:3
Corn	11.67	1.85	0.24	0.00	0.00	25.16	0.00	60.60	0.48
Cottonseed	28.33	0.89	0.00	0.00	0.00	13.27	0.00	57.51	0.00
Crambe	20.70	0.70	2.09	0.80	1.12	18.86	58.51	9.00	6.85
Peanut	11.38	2.39	1.32	5.52	1.23	48.28	0.00	31.95	0.93
Rapeseed	3.49	0.85	0.00	0.00	0.00	64.40	0.00	22.30	8.23
Soybean	11.75	3.15	0.00	0.00	0.00	23.26	0.00	55.53	6.31
Sunflower	6.08	3.26	0.00	0.00	0.00	16.93	0.00	73.73	0.00

methoxide, and followed by each one of the three organic transesterification steps of virgin soybean oil.

## MATERIALS AND METHODS

### Selection of Reactants and Operating Conditions

The source of triglycerides was chosen considering its composition, which should include relatively, high percentage of monounsaturated fatty acids (C16: 1, C18: 1), low proportion of polyunsaturated acids (C18: 2, C18: 3) and adequate content of saturated fatty acids (C16: 0, C18: 0) (Betiku and Adepoju, 2013). Because virgin soybean oil is one of the most abundant oils in Mexico, and its composition is a feasible candidate for this process (Table 1), it was selected for the transesterification experiments.

Methanol (CH<sub>3</sub>OH) was chosen as the reactant for the transesterification, and the inorganic agent was sodium hydroxide (NaOH). These two compounds form sodium methoxide, following an inorganic reaction, prior to be added to the triglycerides source. An important factor in the transesterification process is the initial mixing of the methoxide and the triglyceride (TG) phases (Noureddini and Zhu, 1997). To avoid formation of two liquid layers, the triglyceride and the methoxide solution were preheated prior to mixing.

Mechanical agitation was continuously applied to maintain uniform concentration of the reactants. According to Darnoko and Cheryan (2000), between 120 and 600 rpm there is not limitation to mass transfer; therefore, agitation rate has been set at 250 rpm to avoid foams formation.

Theoretically, three molecules of methanol are required by one molecule of triglyceride to produce three molecules of FAME and one molecule of glycerol. As common practice, excess of alcohol is used in the production of FAME to ensure that the oil or fats will be completely converted to esters. The yield to the FAME is increased proportionally to the excess of alcohol to a maximum point; however, increasing the amount of alcohol beyond this value will not improve the yield, but it will improve the cost of alcohol recovery (Leung and Guo, 2006). Additionally, the molar ratio is associated with the type of catalyst used, the most used ratio in alkaline medium is 6:1 (Zhang et al., 2003). Regarding the reaction time, an excessive increase in the reaction time will result in a significant reduction in the yield of

the product since some FAME will form soaps (Eevera et al., 2009). The temperature clearly influences performance; higher temperature can decrease the viscosity of the oil resulting in an increase in the reaction ratio and reduced reaction time. Simultaneously, if the temperature increases beyond the optimum, the yield will decrease, because at higher temperature the triglyceride saponification reaction accelerates. Finally, the yield to FAME increases proportionally to the amount of alkali supplied up to 1.5wt%; if more alkali is supplied, then saponification reactions are favored (Leung et al., 2006). One measure of the quality of the FAME produced is reflected by the density, which is compared with the EN14214 standard according to Bulla-Pereira (2014).

Samples of transesterification products were obtained following a 2<sup>4-1</sup> fractional factorial design of experiments, with five replicas at the central point to estimate standard deviation (Ogunnaike, 2009) (Table 2). Part of the methanol necessary as reactant was converted into sodium methoxide, measured as (CH<sub>3</sub>OH/TG) ratio, and the rest was blended within the oil, measured as (methanol *in situ*, vol%). The former one is expected to form sodium methoxide using the sodium hydroxide recovered after esters formation. The pH was monitored as response variable, using a potentiometer; in addition, the *yield to FAME*, the (FAME/G) ratio and the final density of FAME were followed (Table 2).

In order to minimize the measurement error and the bias (Ogunnaike, 2009), experimental runs were randomized using the Minitab 17<sup>TM</sup> statistical program; 13 experiments and duplicates were performed following the 2<sup>4-1</sup> design of experiments (see Appendix for the order of experiments). The kinetic constants were calculated following the mass balances up to the time the equilibrium is reached, as it is explained in *Estimation of the Kinetics Rates' Constants* subsection.

### Reaction Pathways

The transesterification reactions of triglycerides follow a sequence of complex inorganic-organic mechanisms. This section describes the reactions involved, considering them ionic ones and with formation of an activated complex intermediate. All the samples were prepared in batch reactors (flasks) at the conditions proposed in the design of experiments.

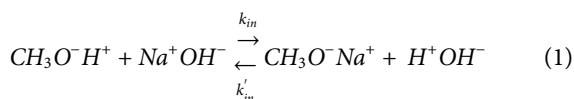
### Synthesis of Sodium Methoxide

First stage consists of the synthesis of sodium methoxide (Eq. 1), by the inorganic reaction of methanol (supplied by J.T. Baker,

**TABLE 2** | Fractional factorial  $2^{4-1}$  design of experiments.

Factor	Low level	High level	Responses
Temperature, °C	46	52	final pH
CH <sub>3</sub> OH/TG ratio	3:1	7:1	yield to FAME, g
NaOH/TG ratio	12:100	4:100	FAME/G ratio
Methanol in situ vol%	10	30	Final density of FAME, g/cm <sup>3</sup>

purity 99.7 mol%) and sodium hydroxide (supplied by Merk-Millipore, purity 99.97 mol%), under constant agitation (250 rpm), at 48°C and room pressure. In order to displace equilibrium to the right-hand side ( $K_{eq} = 0.043$ , at 48°C), methanol was supplied in excess of about 7:1 with respect to sodium hydroxide, as suggested in previous works (Marchetti et al., 2007; Zhang et al., 2003). This reaction (Eq. 1) contemplates the important formation of a water molecule, which remains in the solution.



### Sequential Steps of Transesterification

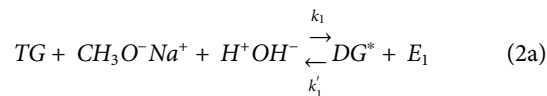
The second stage starts with addition of the solution of sodium methoxide to the preheated soybean oil (TG) and methanol *in situ*, as the first of the three steps described below. The solution of sodium methoxide and the blend of TG and methanol *in situ* (see Table 2) are homogeneous solutions; this situation prevails after the addition of the sodium methoxide solution, therefore there are not mass transfer problems, and the reacting system is controlled by kinetics. As reactions proceed, a second phase appears, which is identified as glycerol (G); this product does not participate in any reaction, so its presence does not affect the mass transfer behavior of the reacting system.

The addition of the sodium methoxide solution to the blend of TG and methanol *in situ* provokes three sequential reaction steps (described below), which form the esters as desired products and sodium hydroxide as by-product. This sodium hydroxide is the one available to be converted, *in situ*, into sodium methoxide by reacting with the methanol *in situ*. Steps of the transesterification mechanism were developed earlier (Mumtaz et al., 2017); however, in this work the concept of “formation of an activated complex” is used rather than the “homogeneous catalysis” one.

#### Formation of the First Ester

The generation of the following kinetic model allows to involve the chemical species in the system as ions, which facilitates the monitoring of the performance of the reaction in each ester, not only in the final production of FAME. In addition to demonstrating the generation and consumption of sodium hydroxide throughout the reaction as one more reagent, not properly as a catalyst that does not intervene in the reaction, allowing to propose the formation of sodium methoxide *in-situ*. Formation of the first ester involves two sequential reactions:

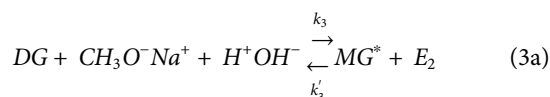
Firstly, one methoxide attacks the intermediate glyceride, forming  $E_1$  and the activated complex ( $DG^*$ ), which stabilizes with the water in the media (Eq. 2a), by forming two tetrahedral oxygens. The sequential reaction is the instantaneous decomposition of the  $DG^*$  into the diglyceride (DG) and a molecule of sodium hydroxide (Eq. 2b).



#### Formation of the Second Ester

Analogous to the formation of  $E_1$ , formation of  $E_2$  involves two sequential reactions:

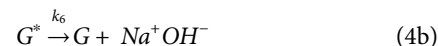
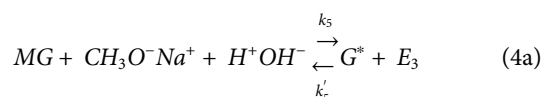
The first reaction is carried out by the attack of one methoxide to one of the terminal glycerides, forming  $E_2$  and the activated complex ( $MG^*$ ), which stabilizes with the water in the media (Eq. 3a) by forming two tetrahedral oxygens. The sequential reaction is the instantaneous decomposition of the  $MG^*$  into the monoglyceride (MG) and one molecule of sodium hydroxide (Eq. 3b).



#### Formation of the Third Ester

Analogous to the formation of  $E_1$  and  $E_2$ , formation of  $E_3$  involves two sequential reactions:

Finally, the last ester formation is carried out by the first reaction, attack of one methoxide to the other terminal glyceride, forming  $E_3$  and the transition compound ( $G^*$ ), which stabilizes with the water in the media (Eq. 4a) by forming two tetrahedral oxygens. The sequential reaction is the instantaneous decomposition of the  $G^*$  into the glycerol (G) and the third sodium hydroxide molecule (Eq. 4b).



### Mass Balances of the Transesterification Pathways

The reaction pathways described for the inorganic formation of sodium methoxide (Eq. 1) and the sequential reaction steps of the triglyceride transesterification (Eqs. 2a, 4b), were modeled by classic mass balances for batch reactors (Eq. 5), developing nine kinetic Eqs. 6–14.

$$\frac{d[C]}{dt} = -f_c(\vec{C}; \vec{k}) \quad (5)$$

$$\begin{aligned} \frac{d[H^+]}{dt} = \frac{d[CH_3O^-]}{dt} = & (k'_{in} - k_{in})([CH_3O^-][Na^+][H^+][OH^-] - \\ & k_1[TG][CH_3O^-][Na^+][H^+][OH^-] + k'_1[DG^*][E_1] - \\ & k_3[DG][CH_3O^-][Na^+][H^+][OH^-] + k'_3[MG^*][E_2] - \\ & k_5[MG][CH_3O^-][Na^+][H^+][OH^-] + k'_5[G^*][E_3]) \end{aligned} \quad (6)$$

$$\begin{aligned} \frac{d[DG^*]}{dt} = & k_1[TG][CH_3O^-][Na^+][H^+][OH^-] - k'_1[DG^*][E_1] \\ & - k_2[DG^*] \end{aligned} \quad (7)$$

$$\begin{aligned} \frac{d[MG^*]}{dt} = & k_3[DG][CH_3O^-][Na^+][H^+][OH^-] - k'_3[MG^*][E_2] \\ & - k_4[MG^*] \end{aligned} \quad (8)$$

$$\begin{aligned} \frac{d[G^*]}{dt} = & k_5[MG][CH_3O^-][Na^+][H^+][OH^-] - k'_5[G^*][E_3] \\ & - k_6[G^*] \end{aligned} \quad (9)$$

$$\frac{d[G]}{dt} = k_6[G^*] \quad (10)$$

$$\frac{dE_2}{dt} = \frac{d[DG^*]}{dt} = k_1[DG^*][Na^+][H^+][OH^-] - k'_1[E_1][DG^*] \quad (11)$$

$$\frac{dE_1}{dt} = \frac{d[MG^*]}{dt} = k_3[MG^*][Na^+][H^+][OH^-] - k'_3[E_2][MG^*] \quad (12)$$

$$\frac{dE_3}{dt} = \frac{d[G^*]}{dt} = k_5[G^*][Na^+][H^+][OH^-] - k'_5[E_3][G^*] \quad (13)$$

$$\begin{aligned} \frac{d[Na^+]}{dt} = \frac{d[OH^-]}{dt} = & (k'_{in} - k_{in})([CH_3O^-][Na^+][H^+][OH^-]) - \\ & k_1[TG][CH_3O^-][Na^+][H^+][OH^-] + k'_1[DG^*][E_1] + \\ & k_2[DG^*] - k_3[DG][CH_3O^-][Na^+][H^+][OH^-] - k'_3[MG^*][E_2] + k_4[MG^*] - \\ & k_5[MG][CH_3O^-][Na^+][H^+][OH^-] + k'_5[G^*][E_3] + k_6[G^*] \end{aligned} \quad (14)$$

Because of instantaneous lifetime of the transition compounds ( $DG^*$ ,  $MG^*$ ,  $G^*$ ), their concentrations, are assumed to be pseudo-stationary. Thus, the instantaneous concentrations of these compounds (Eqs. 15–17) are obtained from their balances (Eqs. 7–9) in terms of the balance of hydrogen ions (Eq. 6).

$$[DG^*] = \frac{k_1[TG] \frac{1}{(k'_{in} - k_{in})} \frac{d[H^+]}{dt}}{k'_1[E_1]} \quad (15)$$

$$[MG^*] = \frac{k_3[DG] \frac{1}{(k'_{in} - k_{in})} \frac{d[H^+]}{dt}}{k'_3[E_2]} \quad (16)$$

$$[G^*] = \frac{k_5[MG] \frac{1}{(k'_{in} - k_{in})} \frac{d[H^+]}{dt}}{k'_5[E_3]} \quad (17)$$

Substituting the concentrations of the intermedium compounds, kinetic expressions in terms of the change of  $pH$  along the reaction time are obtained (Eqs. 18–20).

$$\frac{d[TG]}{dt} = k_1[TG] \frac{1}{(k'_{in} - k_{in})} \frac{d[H^+]}{dt} - k'_1[DG^*][E_1] \quad (18)$$

$$\frac{d[DG]}{dt} = k_3[DG] \frac{1}{(k'_{in} - k_{in})} \frac{d[H^+]}{dt} - k'_3[MG^*][E_2] \quad (19)$$

$$\frac{d[MG]}{dt} = k_5[MG] \frac{1}{(k'_{in} - k_{in})} \frac{d[H^+]}{dt} - k'_5[G^*][E_3] \quad (20)$$

This model (Eqs. 6, 18–20) is used to estimate the kinetic constants of the proposed pathways of transesterification of virgin soybean oil (TG) with sodium methoxide; the latter one formed by the reaction of methanol and sodium hydroxide. It has to be noticed that, taking the point of view from Process Engineering, the mass balances necessary to be included are only the ones independent by stoichiometry. Checking the reactions, it is possible to identify one independent inorganic reaction (Eq. 6), and three independent organic ones. Therefore, after simplification of the mass balance equations for the organic reactions, we need only three of them, which are in Eqs. 18–20.

## RESULTS AND DISCUSSION

The statistic responses were measured for each experiment and statistical analysis were performed for each factor involved in the design of experiments. Later, applying classic mass balances for the interest molecules, the kinetic model was evaluated and validated. Finally, kinetic constants were estimated and used to simulate the reactions with Eqs. 18–20.

### Experimental Evaluation

The design of experiments described in *Selection of Reactants and Operating Conditions* Section was run in random order (Appendix Table A1) obtaining the results in Table 3. The ANOVA (Appendix Table A2) strongly suggests that there is influence of the factors on the measured responses ( $p$ -value < 0.00001, for all factors-response combinations); therefore, deeper analysis was performed.

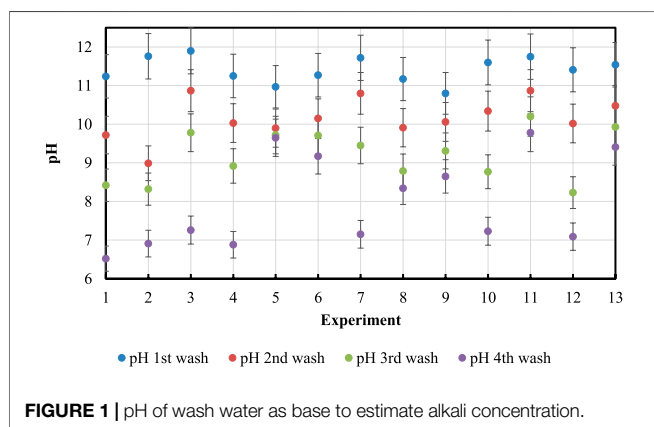
In order to follow the behavior of the sodium hydroxide, the pH of the first wash of the esters blend was measured (Figure 1); in all the experiments its values were observed between 10 and 12. This value can be used to calculate the concentration of  $pOH^-$  ions, which is consequence of the amount of alkaline species absorbed by the FAME. Besides, this amount of species is a reply to two experimental factors, mainly, methanol *in situ* and initial amount of supply of sodium hydroxide to prepare the sodium methoxide *extra situ*.

The statistical analysis of this information was carried out using a Pareto diagram (Figure 2), which shows the effect of the different combinations of factors in the pH response. As it can be seen, in addition to NaOH, the combination with the temperature at which transesterification is carried out and the methanol *in situ* (directly fed to the reaction), influence the amount of wash water necessary to neutralize the FAME. This track was particularly useful, since for this design of experiments it was proposed to add excess of methanol *in situ* and, meanwhile, decrease the amount of methoxide prepared *extra situ*; so that the proposed reaction mechanism could be verified; here a chain reaction has been carried out.

**TABLE 3** | Experimental results from the  $2^{4-1}$  design of experiments.

Experiment	final pH	FAME, g	FAME/G, ratio	FAME density, g/cm <sup>3</sup>
1	11.23	10.0	3.33	0.8491
2	11.76	10.1	6.31	0.8713
3	11.90	10.2	6.37	0.8650
4	11.25	10.0	6.67	0.8604
5	10.97	9.1	2.46	0.8436
6	11.27	10.4	3.47	0.8605
7	11.72	10.0	6.25	0.8669
8	11.17	9.6	3.31	0.8527
9	10.08	10.0	7.69	0.8739
10	11.6	10.0	5.88	0.8700
11 <sup>a</sup>	11.75	9.2	—	—
12	11.41	10.0	6.67	0.8613
13	11.54	10.8	5.40	0.8590

<sup>a</sup>Experiment number 11 leads to soap formation, therefore it was not considered in the analysis.



By measuring the (FAME/G) product ratio, it was found that its value (6/1) agrees with the literature (Mumatz et al., 2017); therefore, in this range of operating conditions good FAME production is achieved (Figure 3). Following the present design of experiments, the highest yield was obtained in experiment 9, which is the maximum point.

The next response measured was the final density of FAME, which is affected by excess of methanol fed, and by the amount of NaOH (Figure 4). This behavior was expected since methanol is fed *in situ* without reacting completely, and there is not a removal stage as the distillation proposed in the literature (Zhang et al., 2003); therefore, some excess of methanol could be present within the mixture of methyl esters.

After this analysis, it is noted that the temperature interval used was too short to exhibit any significant effect. Therefore, it was considered that the results obtained do not correspond to different temperatures, but are duplicate experiments at the same average temperature of 48°C. With this, the ability to estimate activation energies is lost, but precision in mass balances is increased.

## Mass Balances of the Transesterification Process

Results from the 12 experiments described previously were introduced to the mass balances (22–35), here molar reaction advances ( $\varepsilon_k$ ) were

evaluated for each chemical entity involved in the process. The aim of this section is to estimate the amounts of reaction, in terms of moles, preserving the convergence in mass balances.

Taking as example the experiment with the highest yield to FAME (Exp. 9, Figure 3), solving mass balances in Table 4, and using the global conversion of the triglyceride,  $\xi_{TG} = 0.98$ , the first reaction advance is calculated (Eq. 36). By stoichiometry, the five advances related to esterification reactions are obtained (Eq. 37). These advances are used to solve mol balances (26–35).

$$\varepsilon_1 = TG_0 * \xi_{TG} = 0.0500 \text{ mol/batch} * 0.98 = 0.0490 \text{ mol/batch} \quad (36)$$

$$\varepsilon_1 = \varepsilon_2 = \varepsilon_3 = \varepsilon_4 = \varepsilon_5 = \varepsilon_6 = 0.0490 \text{ mol/batch} \quad (37)$$

Progress of sodium methoxide reaction can be followed by measuring pH (Eq. 38) and using the definition of measure of acidity (Eq. 39); this equivalence allows to determinate ( $OH^-$ ) concentration.

$$pH = -\log[H^+] \quad (38)$$

$$pH + pOH = 14 \quad (39)$$

Experimental value of the pH, measured prior to the washing step, was 10.08. Applying (Eq. 39), the value pOH = 3.92 is calculated (Eq. 40) and converted into concentration (Eq. 41). Taking molecular weight of sodium hydroxide, ( $MW_{NaOH} = 40 \text{ g/mol}$ ), and molar fraction of hydroxide in the molecule, ( $\chi_{OH} = 17/40 = 0.425$ ), it is straightforward to calculate sodium hydroxide concentration in the end products (Eq. 42). Once this value is obtained, the balance of sodium hydroxide can be solved from (24), and the advance of the inorganic reaction is calculated (Eq. 43).

$$pOH = 14 - 9.27 = 4.73 \quad (40)$$

$$[OH^-] = 10^{-4.73} = 1.86 \times 10^{-5} M \quad (41)$$

$$[NaOH]_{output} = 1.86 \times 10^{-5} M / 0.425 = 4.37 \times 10^{-5} M \quad (42)$$

$$\begin{aligned} \varepsilon_{in} &= 6.5 \times 10^{-3} \text{ mol/batch} + \varepsilon_2 + \varepsilon_4 + \varepsilon_6 - 4.37 \times 10^{-5} \text{ mol/batch} \\ &= 0.1564 \text{ mol/batch} \end{aligned} \quad (43)$$



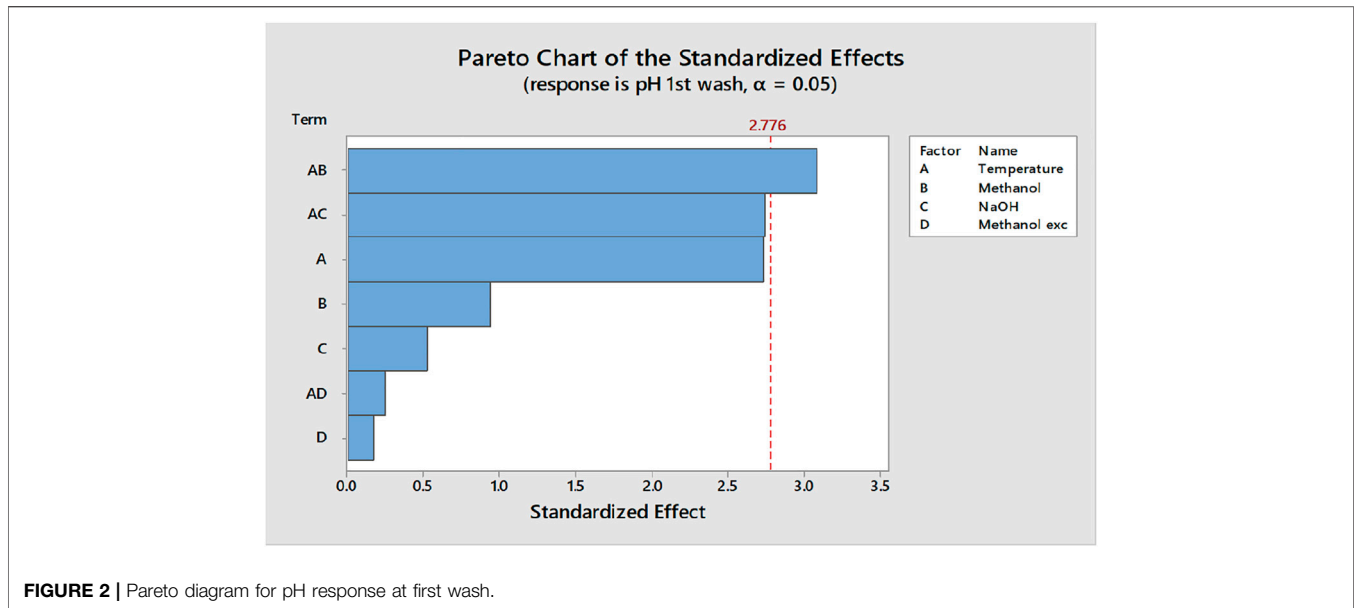


FIGURE 2 | Pareto diagram for pH response at first wash.

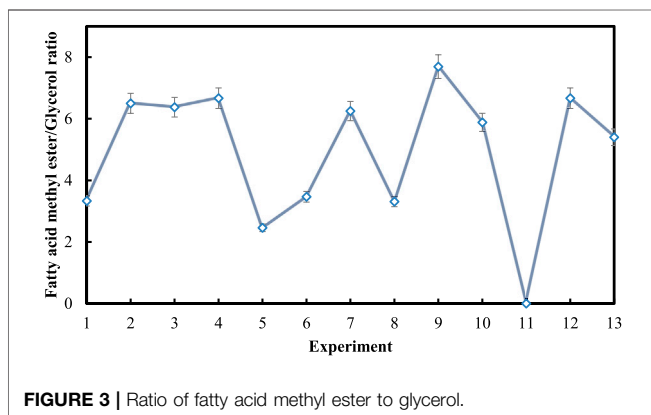


FIGURE 3 | Ratio of fatty acid methyl ester to glycerol.

Then, the mass balance for sodium methoxide (30) is solved and thus the value of balance of water (25) is obtained (Eq. 44); global results are shown in (Table 5, 22a-35).

$$CH_3O^-Na^+ = H_2O = \varepsilon_{in} - \varepsilon_1 - \varepsilon_3 - \varepsilon_5 = 0.0064 \text{ mol / batch} \quad (44)$$

After the advances of reaction were calculated, the theoretical value obtained for the mass balance for glycerol was compared with the experimental weight of the heavier phase, which mainly consists of glycerol. Relative convergence was higher than 99%, excepting in case of the experiment 11; this one was discarded.

## Estimation of the Kinetic Rates' Constants

Once these data are known, the problem of the theoretical project focuses on estimating the value of the kinetic rates' constants for this operating region. According to Leal et al. (1991) and the

expression of Gibbs free energy (Eq. 45a), the value for the reference temperature of 25°C is obtained. Using the actual value of free energy at the reference point (Eq. 45b), the equilibrium constant for the reaction of sodium methoxide can be estimated (Eq. 46). Production of sodium methoxide is carried out at approximately 48°C (321.15 K); this temperature was substituted in (Eq. 46) to obtain the value of the equilibrium constant of the inorganic reaction (Eq. 47).

$$\Delta G^0 = \Delta H^0 - T\Delta S^0 \quad (45a)$$

$$\begin{aligned} \Delta G^0 &= 4780 \text{ J/mol} - (298 \text{ K}) \left( -0.011 \text{ J/mol} \cdot \text{K} \right) \\ &= 4783.278 \text{ J/mol} \end{aligned} \quad (45b)$$

$$K_{in} = \frac{k_{in}}{k'_{in}} = \exp\left(-\frac{\Delta G^0}{R_g T}\right) \quad (46)$$

$$\begin{aligned} K_{in} &= \exp\left(-\frac{4783.278 \text{ J/mol}}{(8.314 \text{ J/mol} \cdot \text{K}) (321.15 \text{ K})}\right) \\ &= \frac{[CH_3O^-][Na^+] \cdot [H^+][OH^-]}{[CH_3O^-][H^+] \cdot [Na^+][OH^-]} = 0.1667 \end{aligned} \quad (47)$$

In order to continue with the estimation of kinetic constants for the simulation of the FAME production process, and based on the reaction schemes presented above, minimization using the Powell's method (included in Matlab<sup>TM</sup>) of the objective function (Eqs. 48a,b) was performed under the only constraint: Kinetic rate constants exhibit positive values (Eq. 48c).

$$\begin{aligned} \min \left\{ \sum_{i=1}^{n_{Exp}} \left[ \left( y_{FAME_{Exp}} - y_{FAME_{Pred}} \right)_i^2 \right. \right. \\ \left. \left. + \left( \left( \frac{FAME}{G} \right)_{exp} - \left( \frac{FAME}{G} \right)_{pred} \right)_i^2 \right] \right\} \end{aligned} \quad (48a)$$

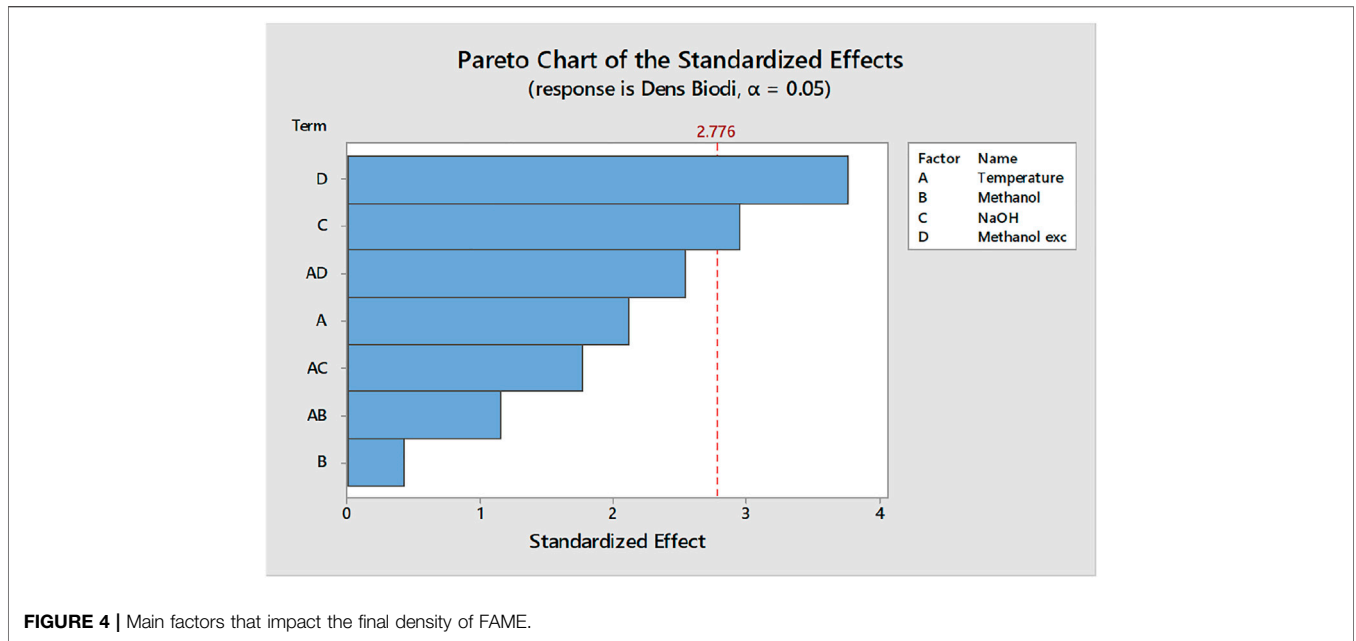


**FIGURE 4** | Main factors that impact the final density of FAME.

**TABLE 4** | Values of kinetic rate constants and confidence intervals ( $\alpha \geq 95\%$ ).

Kinetic rate constant	Value	Units
$k_{in}$	$12000 \pm 757$	$(\text{mol} \cdot \text{cm}^{-3})^{-3} \text{s}^{-1}$
$k'_{in}$	$400 \pm 23$	$(\text{mol} \cdot \text{cm}^{-3})^{-3} \text{s}^{-1}$
$k_1$	$2650 \pm 109$	$(\text{mol} \cdot \text{cm}^{-3})^{-4} \text{s}^{-1}$
$k'_1$	$0.34 \pm 0.02$	$(\text{mol} \cdot \text{cm}^{-3})^{-1} \text{s}^{-1}$
$k_2$	$15 \pm 0.6$	$\text{s}^{-1}$
$k_3$	$11500 \pm 197$	$(\text{mol} \cdot \text{cm}^{-3})^{-4} \text{s}^{-1}$
$k'_3$	$0.16 \pm 0.03$	$(\text{mol} \cdot \text{cm}^{-3})^{-1} \text{s}^{-1}$
$k_4$	$27 \pm 0.31$	$\text{s}^{-1}$
$k_5$	$7540 \pm 151$	$(\text{mol} \cdot \text{cm}^{-3})^{-4} \text{s}^{-1}$
$k'_5$	$0.28 \pm 0.02$	$(\text{mol} \cdot \text{cm}^{-3})^{-1} \text{s}^{-1}$
$k_6$	$13.6 \pm 0.15$	$\text{s}^{-1}$

$$\leftrightarrow \min \left[ \sum_{i=1}^{n_{Exp}} [\Psi_{FAME} + \Psi_{Ratio}] \right] \quad (48b)$$

Subjected to:

$$k_1, \dots, k_6 \geq 0 \quad (48c)$$

Here  $\Psi_{FAME}$  and  $\Psi_{Ratio}$  are the quadratic errors of estimation of yield to FAME and the ratio of the yield to products, respectively.

The estimation of the kinetic rate constants depends on precision of measurement of the yields to FAME and the ratio (Figure 2) of products. Applying the usual methodology of error propagation (Eq. 49), in order to estimate confidence intervals ( $\alpha \geq 95\%$ ), the propagated errors of the six kinetic rate constants were calculated (Table 4).

$$\Delta k_m = \left| \left( \frac{\partial k}{\partial \Psi_{FAME}} \right)_m \right| \Delta \Psi_{FAME} + \left| \left( \frac{\partial k}{\partial \Psi_{Ratio}} \right)_m \right| \Delta \Psi_{Ratio} \quad (49)$$

## Simulation of the Transesterification Reactions Pathways

The mean values of the kinetic rate constants (Table 5) were used to simulate the evolution of triglyceride consumption and FAME production for all experiments; an example is given for the best experiment (# 9, Figure 5).

As consequence of the good conversion of TG, DG and MG, production of FAME (Figure 5) shows continuous growing trend; for this experiment calculation of the yield to FAME (Eq. 50) agrees with the results observed for TG conversion and with data reported in literature (Vicente et al., 2004; Marchetti et al., 2007).

$$y_{FAME} = \frac{\sum \text{esters}}{TG_0} * 100 \Rightarrow y_{FAME} = \frac{0.0494219}{0.0500000} * 100 = 98.84 \text{ wt. \%} \quad (50)$$

In fact, for this experiment conversion of TG follows first order trend (Figure 5); also, conversion is practically complete. The same is true for DG and MG, which is confirmed by the yield to G (Eq. 51).

$$\frac{G_{pred}}{G_{exp}} = \frac{0.01847}{0.02189} = 0.8438 \quad (51)$$

The kinetic constants estimated (Table 4) were, also, used to simulate the evolution of sodium methoxide (Figure 6). It is interesting to see that formation of sodium hydroxide (inorganic reaction in 1) is taking place along the whole experimental time; therefore, sodium hydroxide is playing the role of reactant rather than acting as catalyst. Moreover, it is not necessary to “prepare” a batch of the basic solution prior to addition to the triglyceride, because the inorganic reaction is able to take place simultaneously to the transesterification one, as soon as sodium hydroxide is recovered and there is methanol

**TABLE 5** | Solution of mass balances for experiment 9.

Compound	$F_1$ (moles/batch)	$F_2$ (moles/batch)	
TG	0.05	$0.05 - \varepsilon_1$	(22)
$CH_3OH$	0.5	$0.5 - \varepsilon_{in}$	(23)
NaOH	$6.25 \times 10^{-3}$	$6.5 \times 10^{-3} - \varepsilon_{in} + \varepsilon_2 + \varepsilon_4 + \varepsilon_6$	(24)
$H_2O$	0	$\varepsilon_{in} - \varepsilon_1 - \varepsilon_3 - \varepsilon_5$	(25)
G	0	$\varepsilon_6$	(26)
$E_1$	0	$\varepsilon_3$	(27)
$E_2$	0	$\varepsilon_1$	(28)
$E_3$	0	$\varepsilon_5$	(29)
$CH_3O^-Na^+$	0	$\varepsilon_{in} - \varepsilon_1 - \varepsilon_3 - \varepsilon_5$	(30)
DG	0	$0 = \varepsilon_2 - \varepsilon_3$	(31)
MG	0	$0 = \varepsilon_4 - \varepsilon_5$	(32)
$TG^*$	0	$0 = \varepsilon_1 - \varepsilon_2$	(33)
$DG^*$	0	$0 = \varepsilon_3 - \varepsilon_4$	(34)
$MG^*$	0	$0 = \varepsilon_5 - \varepsilon_6$	(35)
TG	0.05	$0.05 - \varepsilon_1 = 0.0010$	(22a)
$CH_3OH$	0.5	$0.5 - \varepsilon_{in} = 0.03436$	(23a)
NaOH	$6.25 \times 10^{-3}$	$6.5 \times 10^{-3} - \varepsilon_{in} + \varepsilon_2 + \varepsilon_4 + \varepsilon_6 = 0.0064$	(24a)
$H_2O$	0	$\varepsilon_{in} - \varepsilon_1 - \varepsilon_3 - \varepsilon_5 = 0.0064$	(25a)
G	0	$\varepsilon_6 = 0.0490$	(26a)
$E_1$	0	$\varepsilon_3 = 0.0490$	(27a)
$E_2$	0	$\varepsilon_1 = 0.0490$	(28a)
$E_3$	0	$\varepsilon_5 = 0.0490$	(29a)
$CH_3O^-Na^+$	0	$\varepsilon_{in} - \varepsilon_1 - \varepsilon_3 - \varepsilon_5 = 0.0064$	(30a)
DG	0	$\varepsilon_2 - \varepsilon_3 = 0$	(31a)
MG	0	$\varepsilon_4 - \varepsilon_5 = 0$	(32a)
$DG^*$	0	$\varepsilon_1 - \varepsilon_2 = 0$	(33a)
$MG^*$	0	$\varepsilon_3 - \varepsilon_4 = 0$	(34a)
$G^*$	0	$\varepsilon_5 - \varepsilon_6 = 0$	(35a)

available in the reacting mixture (see reaction mechanism, Eqs. 2–4).

Finally, it was found that there is inverse correlation between the yield to FAME and the amount of water necessary for the purification of the FAME; the impact of each factor on the yield to FAME (Eq. 52), shows that the amount of sodium hydroxide added at the beginning is the only significant one.

$$\begin{aligned}
 H_2O_{wash} (ml) = & 462.7 - 9.167 * Temperature + 33.89 * Methanol \\
 & + 53.57 * NaOH - 24.25 * Methanol_{exc} \\
 & - 0.5556 * Temperature * Methanol \\
 & + 0.5000 * Temperature * Methanol_{exc} \\
 & - 22.50 * CtPt
 \end{aligned}
 \tag{52}$$

## CONCLUSION

This study develops a novel way to estimate the reaction rates for the transesterification of triglycerides, with the knowledge of intermediate compounds along the reaction time. It was emphasized that production and consumption of sodium methoxide show that the inorganic reaction is taking place along the whole experimental time; therefore, sodium hydroxide is playing the role of reactant rather than acting as catalyst. Also, the mechanism found that sodium hydroxide never interacts with triglyceride; in contrast, it is regenerated after the methoxide

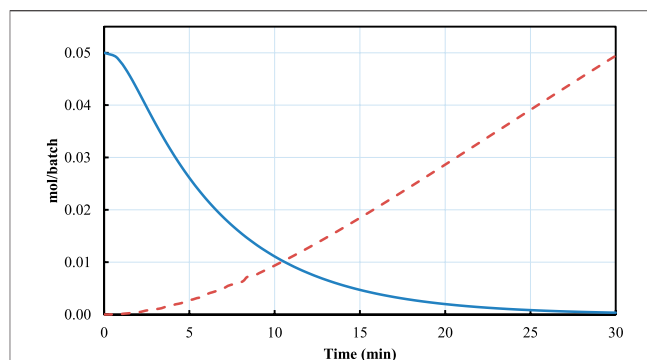


**FIGURE 5** | Theoretical prediction of FAME production --- and TG consumption, experiment # 9.

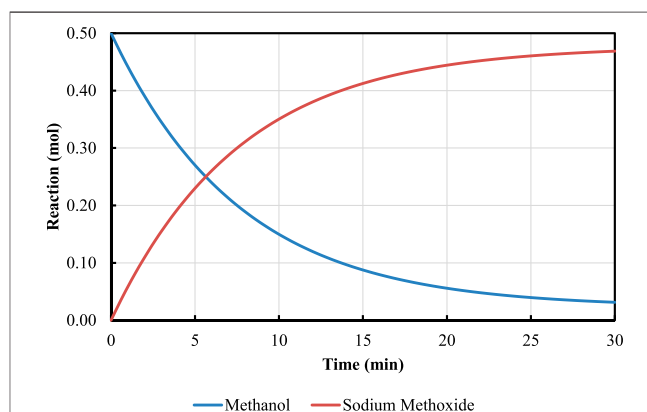


**FIGURE 6** | Consumption of methanol and production of the methoxide with time, experiment # 9.

attacks the carbonyl oxygen of the organic compounds TG, DG and MG. Additionally, it is not necessary to “prepare” a batch of the basic solution prior to addition to the triglyceride, because the inorganic reaction is able to take place simultaneously to the transesterification one, as soon as sodium hydroxide is recovered and there is methanol available in the reacting mixture. This point of view allows reducing the amount of the NaOH in the feed, which makes FAME production friendlier with the environment.

## DATA AVAILABILITY STATEMENT

The original contributions presented in the study are included in the article/Supplementary Material, further inquiries can be directed to the corresponding author.

## AUTHOR CONTRIBUTIONS

All authors listed have made a substantial, direct, and intellectual contribution to the work and approved it for publication.



## ACKNOWLEDGMENTS

MAPM thanks postgraduate studies scholarship 861765 from Consejo Nacional de Ciencia y Tecnología

(CONACYT). GJG, RHA and RMY greatly appreciate research system grants (SNI-CONACYT). Financial support provided by CIC-UMSNH (Project 20.20) is greatly appreciated.

## REFERENCES

- Betiku, E., and Adepoju, T. F. (2013). Methanolysis Optimization of Sesame (*Sesamum indicum*) Oil to BD and Fuel Quality Characterization. *Int. J. Energ. Environ. Eng.* 4, 9. doi:10.1186/2251-6832-4-9
- Bulla-Pereira, E. A. (2014). *Diseño del proceso de producción de biodiesel a partir de aceites de fritura*. Colombia: Bogotá.
- Darnoko, D., and Cheryan, M. (2000). Kinetics of palm Oil Transesterification in a Batch Reactor. *J. Amer Oil Chem. Soc.* 77, 1263–1267. doi:10.1007/s11746-000-0198-y
- Everera, T., Rajendran, K., and Saradha, S. (2009). Biodiesel Production Process Optimization and Characterization to Assess the Suitability of the Product for Varied Environmental Conditions. *Renew. Energ.* 34, 762–765. doi:10.1016/j.renene.2008.04.006
- Granjo, J. F. O., and Oliveira, N. M. C. (2015). Process Simulation and Techno-Economic Analysis of the Production of Sodium Methoxide. *Ind. Eng. Chem. Res.* 55, 156–167. doi:10.1021/acs.iecr.5b02022
- Leal, J. P., de Matos, A. P., and Simões, J. A. M. (1991). Standard Enthalpies of Formation of Sodium Alkoxides. *J. Organomet. Chem.* 403, 1–10. doi:10.1016/0022-328x(91)83081-e
- Leung, D. Y. C., and Guo, Y. (2006). Transesterification of Neat and Used Frying Oil: Optimization for Biodiesel Production. *Fuel Process. Technol.* 87, 883–890. doi:10.1016/j.fuproc.2006.06.003
- Leung, D. Y. C., Koo, B. C. P., and Guo, Y. (2006). Degradation of Biodiesel under Different Storage Conditions. *Bioresour. Technol.* 97, 250–256. doi:10.1016/j.biortech.2005.02.006
- Marchetti, J. M., Miguel, V. U., and Errazu, A. F. (2007). Possible Methods for Biodiesel Production. *Renew. Sustain. Energ. Rev.* 11, 1300–1311. doi:10.1016/j.rser.2005.08.006
- Mendecka, B., Lombardi, L., and Koziol, J. (2020). Probabilistic Multi-Criteria Analysis for Evaluation of Biodiesel Production Technologies from Used Cooking Oil. *Renew. Energ.* 147, 2542–2553. doi:10.1016/j.renene.2017.05.037
- Mumtaz, M. W., Adnan, A., Mukhtar, H., Rashid, U., Danish, M., and Kalam Azad, A. (2017). “Fatty Acid Methyl Ester Production through Chemical and Biochemical Transesterification: Trends, Technicalities, and Future Perspectives,” in *Clean Energy for Sustainable Development: Comparisons and Contrasts of New Approaches*. Chapter 15. Editors M G. Rasul and S C. Sharma (London UK: Edit. Academic Press (Elsevier Inc)).
- Noureddini, H., and Zhu, D. (1997). Kinetics of Transesterification of Soybean Oil/frac of Soybean Oil. *J. Amer Oil Chem. Soc.* 74, 1457–1463. doi:10.1007/s11746-997-0254-2
- Ogunnaike, B. A. (2009). *Random Phenomena: Fundamentals of Probability and Statistics for Engineers*. New York: CRC Press.
- Rincón, L. E., Jaramillo, J. J., and Cardona, C. A. (2014). Comparison of Feedstocks and Technologies for Biodiesel Production: An Environmental and Techno-Economic Evaluation. *Renew. Energ.* 69, 479–487. doi:10.1016/j.renene.2014.03.058
- Sharma, Y. C., Singh, B., and Upadhyay, S. N. (2008). Advancements in Development and Characterization of Biodiesel: A Review. *Fuel* 87, 2355–2373. doi:10.1016/j.fuel.2008.01.014
- Silitonga, A. S., Shamsuddin, A. H., Mahlia, T. M. I., Milano, J., Kusumo, F., Siswanto, J., et al. (2020). Biodiesel Synthesis from Ceiba Pentandra Oil by Microwave Irradiation-Assisted Transesterification: ELM Modeling and Optimization. *Renew. Energ.* 146, 1278–1291. doi:10.1016/j.renene.2019.07.065
- Vicente, G., Martínez, M., and Aracil, J. (2004). Integrated Biodiesel Production: a Comparison of Different Homogeneous Catalysts Systems. *Bioresour. Technol.* 92, 297–305. doi:10.1016/j.biortech.2003.08.014
- Vinoth Kanna, I., Devaraj, A., and Subramani, K. (2018). Bio Diesel Production by Using Jatropha: the Fuel for Future. *Int. J. Ambient Energ.* 41, 289–295. doi:10.1080/01430750.2018.1456962
- Zhang, Y., Dubé, M. A., McLean, D. D., and Kates, M. (2003). Biodiesel Production from Waste Cooking Oil: 1. Process Design and Technological Assessment. *Bioresour. Technol.* 89, 1–16. doi:10.1016/s0960-8524(03)00040-3

**Conflict of Interest:** UG Editor. Frontiers in Chemical Engineering As responsible of the manuscript sent to the Special Issue about the Research Topic “Sustainable Process and Product Design,” I sent the original list of authors. However, I made a mistake including the name “A. Dutta” prior to ask him if he agreed to be listed as co-author. As consequence, Dutta asked to be removed from the list of authors, which should be my responsibility, also. We are sending the revised version of the manuscript; the list of authors does not contain the name “A. Dutta.” As correspondence author, and chief of the research project, I take the responsibility of this change. If there are some additional requests to be considered, please let me know. Best regards, RM-Y Correspondence author.

The remaining authors declare that the research was conducted in the absence of any commercial or financial relationships that could be construed as a potential conflict of interest.

Copyright © 2021 Pérez-Méndez, Jiménez-García, Huirache-Acuña and Maya-Yescas. This is an open-access article distributed under the terms of the Creative Commons Attribution License (CC BY). The use, distribution or reproduction in other forums is permitted, provided the original author(s) and the copyright owner(s) are credited and that the original publication in this journal is cited, in accordance with accepted academic practice. No use, distribution or reproduction is permitted which does not comply with these terms.

## GLOSSARY

**DG** Diglyceride

**DG\*** Transition complex formed by an activated diglyceride, a methoxide ion, and a molecule of water

**FAME** Fatty acid methyl esters

**G** Glycerol

**G\*** Transition complex formed by an activated glycerol, a methoxide ion, and a molecule of water

**MG** Monoglyceride

**MG\*** Transition complex formed by an activated monoglyceride, a methoxide ion, and a molecule of water

**TG** Triglyceride

**E<sub>1</sub>** First ester

**E<sub>2</sub>** Second ester

**E<sub>3</sub>** Third ester

**H<sup>+</sup>** Hydrogen ion

**OH<sup>-</sup>** Hydroxide ion

**Na<sup>+</sup>** Sodium ion

**CH<sub>3</sub>O<sup>-</sup>** Methoxide ion

**CtPt** Central point in Eq. 52

$\varepsilon_k$  Degree of advance of the *k*th reaction

$k_{in}$  Kinetic rate constant for inorganic reaction

$k'_{in}$  Kinetic rate constant for reversible inorganic reaction

$k_1$  Kinetic rate constant for triglyceride consumption

$k'_1$  Kinetic rate constant for reversible triglyceride production

$k_2$  Kinetic rate constant for diglyceride production

$k_3$  Kinetic rate constant for diglyceride consumption

$k'_3$  Kinetic rate constant for reversible diglyceride production

$k_4$  Kinetic rate constant for monoglyceride production

$k_5$  Kinetic rate constant for monoglyceride consumption

$k'_5$  Kinetic rate constant for reversible monoglyceride production

$k_6$  Kinetic rate constant for glycerol production

$K_{in}$  Equilibrium constant for inorganic fraction

$\Psi_{FAME}$  Auxiliar variable in the evaluation of error propagation Eqs. 48b, 49

$\Psi_{Ratio}$  Auxiliar variable in the evaluation of error propagation Eqs. 48b, 49

## APPENDIX. EXPERIMENTAL RUNS FROM FATTY ACID METHYL ESTER PRODUCTION

**TABLE A1** | Factorial  $2^{4-1}$  design of experiments with five central points.

Factor/Experiment	Temperature, °C	MetOH/TG, ratio	NaOH/TG, ratio	MetOH <i>in situ</i> , wt%
1	52	3.0	0.40	10
2	49	4.5	0.26	20
3	49	4.5	0.26	20
4	52	6.0	0.12	10
5	52	6.0	0.40	30
6	46	6.0	0.12	30
7	49	4.5	0.26	20
8	46	3.0	0.40	30
9	46	3.0	0.12	10
10	49	4.5	0.26	20
11	46	6.0	0.40	10
12	49	4.5	0.26	20
13	52	3.0	0.12	30

**TABLE A2** | ANOVA of results from the  $2^{4-1}$  design of experiments.

Origin of variations	SS	Degrees of freedom	Estimated F	Probability F	p-value
pH, $\alpha= 0.95$					
Between groups	20849.2249	4	24.1623	3.65	<0.00001
Inside groups	769.615,655	55	—	—	—
Total	21618.8405	59	—	—	—
Yield to BD, $\alpha= 0.95$					
Between groups	20849.2249	4	24.0904	3.65	<0.00001
Inside groups	769.615,655	55	—	—	—
Total	21618.8405	59	—	—	—
(BD/G), $\alpha= 0.95$					
Between groups	20849.2249	4	24.3413	3.65	<0.00001
Inside groups	769.615,655	55	—	—	—
Total	21618.8405	59	—	—	—
Density, $\alpha= 0.95$					
Between groups	20849.2249	4	27.0904	3.65	<0.00001
Inside groups	769.615,655	55	—	—	—
Total	21618.8405	59	—	—	—